

UC San Diego

UC San Diego Previously Published Works

Title

Initial Development toward Non-Invasive Drug Monitoring via Untargeted Mass Spectrometric Analysis of Human Skin

Permalink

<https://escholarship.org/uc/item/4vh54400>

Journal

Analytical Chemistry, 91(13)

ISSN

0003-2700

Authors

Jarmusch, Alan K
Elijah, Emmanuel O
Vargas, Fernando
[et al.](#)

Publication Date

2019-07-02

DOI

10.1021/acs.analchem.8b05854

Peer reviewed

Initial Development toward Non-Invasive Drug Monitoring via Untargeted Mass Spectrometric Analysis of Human Skin

Alan K. Jarmusch,^{†,‡,§} Emmanuel O. Elijah,^{†,‡} Fernando Vargas,^{†,‡} Amina Bouslimani,^{†,‡} Ricardo R. da Silva,^{†,‡,§} Madeleine Ernst,^{†,‡} Mingxun Wang,^{†,‡} Krizia K. del Rosario,[†] Pieter C. Dorrestein,^{*,†,‡,§} and Shirley M. Tsunoda^{*,†}

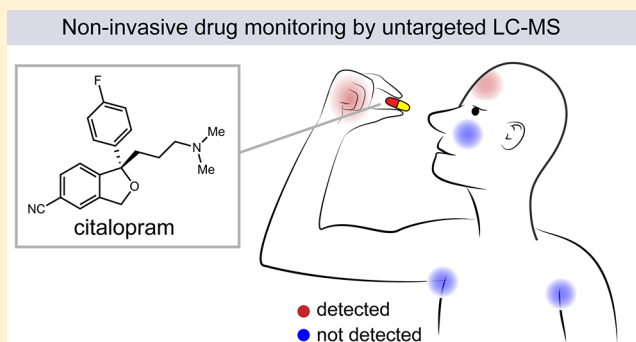
[†]Skaggs School of Pharmacy and Pharmaceutical Sciences, University of California, San Diego, La Jolla, California 92093, United States

[‡]Collaborative Mass Spectrometry Innovation Center, Skaggs School of Pharmacy and Pharmaceutical Sciences, University of California, San Diego, La Jolla, California 92093, United States

[§]NPPNS, Department of Physics and Chemistry, School of Pharmaceutical Sciences of Ribeirão Preto, University of São Paulo, Avenida do Café s/n, 14040-903 Ribeirão Preto, SP, Brazil

S Supporting Information

ABSTRACT: Drug monitoring is crucial for providing accurate and effective care; however, current methods (e.g., blood draws) are inconvenient and unpleasant. We aim to develop a non-invasive method for the detection and monitoring of drugs via human skin. The initial development toward this aim required information about which drugs, taken orally, can be detected via the skin. Untargeted liquid chromatography–mass spectrometry (LC–MS) was used as it was unclear if drugs, known drug metabolites, or other transformation products were detectable. In accomplishing our aim, we analyzed samples obtained by swabbing the skin of 15 kidney transplant recipients in five locations (forehead, nasolabial area, axillary, backhand, and palm), bilaterally, on two different clinical visits. Untargeted LC–MS data were processed using molecular networking via the Global Natural Products Social Molecular Networking platform. Herein, we report the qualitative detection and location of drugs and drug metabolites. For example, escitalopram/citalopram and diphenhydramine, taken orally, were detected in forehead, nasolabial, and hand samples, whereas *N*-acetyl-sulfamethoxazole, a drug metabolite, was detected in axillary samples. In addition, chemicals associated with environmental exposure were also detected from the skin, which provides insight into the multifaceted chemical influences on our health. The proof-of-concept results presented support the finding that the LC–MS and data analysis methodology is currently capable of the qualitative assessment of the presence of drugs directly via human skin.



Human skin is a complex chemical interface between our internal biology and the external world. Chemicals present on the skin originate from many sources, including human metabolism, microbes, behaviors (such as smoking), food, personal care products, the environment, and drugs. In comparison with urine and blood, the chemicals on and in the skin are poorly characterized. Information about the skin metabolome is limited, currently, but appears to be highly reflective of our human behaviors,¹ our built environments,^{2,3} and the objects⁴ with which we interact.

Drug monitoring, for therapeutic, toxic, and adherence purposes, is important for providing accurate and effective care. Therapeutic drug monitoring, critical for narrow therapeutic range drugs, strives to measure the concentration of a drug (or metabolite) in blood to determine if the drug is within a therapeutic window (i.e., sufficient to be effective but not too

much as to cause side effects). Routine blood draws are inconvenient and unpleasant. Adherence testing, intended to objectively determine if prescriptions are being followed, is similarly important in providing optimal care but suffers from being inconvenient (e.g., urine or blood collection).

Drugs and drug metabolites are routinely measured in blood, urine, saliva, and other blood fluids and tissues using mass spectrometry. Mass spectrometry (MS), often coupled to chemical separation methods prior to analysis [e.g., gas chromatography (GC) or liquid chromatography (LC)], has been used to analyze the chemical composition of skin.^{1,4–10} MS detects the mass-to-charge ratio (m/z) of ions, charged

Received: December 19, 2018

Accepted: May 10, 2019

Published: May 10, 2019

versions of neutral molecules, at minute levels (often in the low parts per billion range) and provides structural information using multiple stages of MS (e.g., MS²). Structural information is provided via interpretable fragmentation patterns when excess internal energy is supplied to ions, for example, via collision with gas molecules, i.e., collision-induced dissociation (CID).

There is a prior basis for the detection of drugs via the skin. There have been numerous studies that measured the amount of drug, applied topically, to the skin as well as the depth of drug penetration.^{11–13} Prior studies were commonly performed *in vitro*, or sample collection was performed using tape stripping,⁷ skin scraping,⁹ or punch biopsy.¹⁴ Non-invasive sampling of the skin with swabs is far less invasive, but the following limitations exist currently: sampling is qualitative and user-dependent and provides molecular information only from the outermost layers of the epidermis. With regard to the detection of drugs taken orally, there are only a few studies that suggest that detection is possible from the skin of individuals,^{4,15} but the information present in those studies was not sufficient to understand, in detail, which drugs can be detected via the skin, at which body locations they are detectable, and by which mechanism(s) drugs arrive on or in the skin.

Untargeted MS in its purest form intends to detect all chemicals present in a given sample without knowledge of the composition *a priori*; the metabolome is a subset of those chemicals. In this instance, untargeted MS serves to broadly screen for drugs (and potential metabolites) from the skin, particularly drugs taken orally, without any prior knowledge if certain chemicals are present on the skin. One challenge in performing untargeted MS is the analysis of a large amount of data generated. Our solution is to use the Global Natural Products Social Molecular Networking (GNPS) platform.¹⁶ Molecular networking connects chemicals of similar structure based on MS² data (specifically product ion scans) as similar molecular structures often produce similar MS² fragmentation patterns. The first step is to generate consensus MS² spectra (represented as nodes in the molecular network) by consolidating nearly identical MS² spectra. The consensus MS² spectra are compared and connected via edges and given a cosine score based on the similarity of MS² fragmentation. Grouping of connected consensus spectra (i.e., molecular families) indicates similar fragmentation patterns and a similar molecular structure and reflects chemicals grouped by chemical class. Chemical annotation is performed in GNPS by comparing consensus MS² spectra with reference MS² fragmentation patterns (and supported by accurate measurement of *m/z*). GNPS annotations via spectral reference comparison are considered level 2 (putative annotation based on spectral library similarity) or 3 (putatively characterized compound class based on spectral similarity to known compounds of a chemical class) by the 2007 metabolomics standard initiative.¹⁷

Herein, we report the untargeted MS analysis of skin swabs from the face, hands, and axilla (sampled bilaterally and longitudinally at two clinical visits) of 15 kidney transplant recipients. Specific to our aim in developing a non-invasive method for the detection and monitoring of drugs from the skin, we report (1) the drugs detected by untargeted MS and confirmed using MS² spectra, (2) the locations at which drugs (and metabolites) were detected, and (3) concurrent detection of chemicals associated with environmental exposure and

health. This work describes the initial steps in developing the technology necessary for non-invasive drug monitoring via the skin.

EXPERIMENTAL SECTION

Study Design. Figure 1 illustrates the sample collection and experimental workflow used in this study. Skin samples

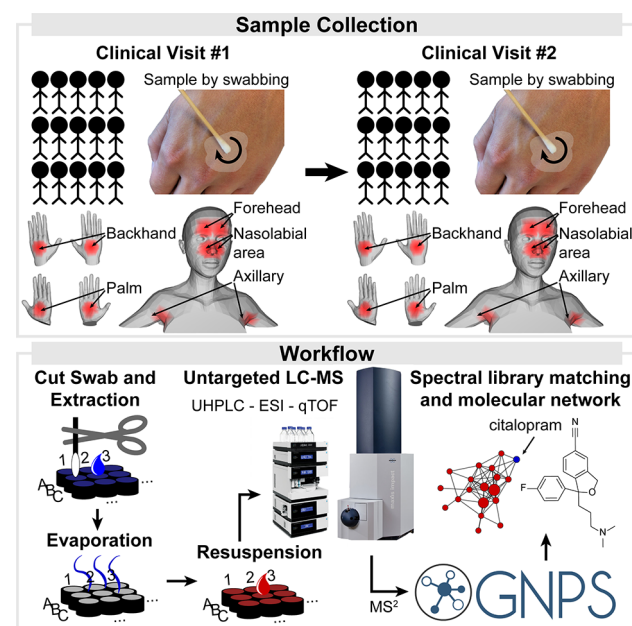


Figure 1. Illustration depicting the sampling of the skin of 15 subjects in 10 locations using a premoistened cotton swab and the subsequent sample handling, data acquisition, and data processing in GNPS.

were collected following an IRB-approved study (University of California, San Diego, IRB 161371) from kidney transplant patients; data from 15 subjects were used in this work. Ten locations on the body (bilateral collection of the forehead, nasolabial area, axillary, backhand, and palm) were sampled per subject at two different times, once during a routine clinic visit (clinic) and once at a subsequent clinical visit (lab). The following numbers of samples per body location were used: $n = 59$ for forehead, $n = 59$ for nasolabial area, $n = 60$ for axillary, $n = 60$ for backhand, and $n = 60$ for palm. Table S1 displays the number of samples collected and included in this work. Metadata pertaining to each sample were collected in accordance with IRB and HIPAA authorization and deidentified and are available in the Supporting Information. The metadata included detailed drug information that is highlighted in the Supporting Information.

Samples. Cotton swabs (Puritan 837 without binders) were soaked in an ethanol/water mixture (1:1) prior to sampling three times to minimize the chemical background observed from the swabs. Swabs moistened with an ethanol–water mixture (1:1) were used to sample the subject’s skin. Samples were collected by rubbing the skin in a circular pattern for ~10 s with moderate, painless, pressure. Swab tips were cut into 96 deep-well plates, sealed, and stored at $-80\text{ }^{\circ}\text{C}$ prior to extraction.

Sample Extraction. Skin swabs in 96 deep-well plates were extracted using 1.2 mL of 100% methanol pipetted using a multichannel pipet. The 96 deep-well plates were capped and sonicated for 300 s. Subsequently, the cap was removed, and

the swabs were removed using a tweezer (rinsing with nanopure water between samples). Aliquots (300 μL) were transferred to 96-well plates and dried via centrifugal evaporation. Samples were resuspended in an acetonitrile–water mixture (1:4) prior to LC–MS analysis. Axillary samples were diluted 10-fold to avoid detector saturation.

Data Acquisition. The skin samples were analyzed using an ultra-high-performance liquid chromatograph (UltiMate 3000, Thermo) coupled to a quadrupole time-of-flight (ToF) mass spectrometer (maXis Impact, Bruker). Chromatographic separation was carried out on a Kinetex C18 1.7 μm , 100 \AA , 2.1 mm (internal diameter) \times 50 mm (length) column (Phenomenex) maintained at 40 $^{\circ}\text{C}$ during separation; 10.0 μL of extract was injected per sample, except for axillary samples, which were injected in 1.0 μL amounts to avoid saturation of the detector. Mobile phase A consisted of water with 0.1% formic acid (v/v), and mobile phase B consisted of acetonitrile with 0.1% formic acid (v/v). Gradient elution was performed as follows: 5% B from 0.0 to 0.5 min, 100% B from 0.5 to 8.0 min, 100% B from 8.0 to 9.0 min, 5% B from 9.0 to 9.1 min, and 5% B from 9.1 to 12.5 min. MS data were collected using data-dependent acquisition. An MS¹ scan from m/z 50 to 1500 at 3 Hz was followed by MS² scans. Fragmentation was produced by stepped collision-induced dissociation (CID) of the five most abundant ions in the prior MS¹ scan. Electrospray ionization, positive mode, was used to convert solution-phase molecules into gas-phase ions for MS analysis using the following source parameters: drying gas, 9.0 L min⁻¹; dry gas heater, 200 $^{\circ}\text{C}$; capillary voltage, 4.5 kV; end plate offset, -0.5 kV; and nebulizer, 2.0 bar. Hexakis(2,2-difluoroethoxy)phosphazene, lock mass standard, was sublimed in the ionization source; the lock mass standard was added such that a signal of $\sim 1 \times 10^5$ was observed.

Data and Code Availability. All MS data (.d and .mzXML files) are publically available via GNPS/MassIVE (massive.ucsd.edu), a public MS data repository, under accession number MSV000081548. All data, files, and Jupyter notebooks (R) used to process data and generate plots are freely available at github.com/alan-jarmusch/UntargetedMS-Drugs-Skin.

Data Processing and Data Analysis. The qToF files (.d) were exported using DataAnalysis (Bruker) as .mzXML files after lock mass correction. Feature finding was performed on MS¹ data in MZmine2,¹⁸ and parameters can be found in the Supporting Information, yielding a data matrix of MS¹ features (i.e., m/z and retention time) and associated peak area. MS² data were analyzed using GNPS.¹⁶ Figures were generated with Jupyter Notebooks (R), Cytoscape,¹⁹ Bruker DataAnalysis, 'ili,²⁰ and formatted in Adobe Illustrator. Additional description of the data analysis methods is present in the Supporting Information.

Molecular Networking and Annotation in GNPS. Molecular networking was performed with networking parameters that reflect a false-discovery rate (FDR) of annotation of $\sim 1\%$; FDR estimation was performed using the Passatutto-GNPS Library Search tool (Figure S1).²¹ The data were filtered by removing all MS² peaks $m/z \pm 17$ of the precursor ion. MS² spectra were window filtered by choosing only the top six peaks in the $m/z \pm 50$ window throughout the spectrum. The data were then clustered with MS-Cluster with a precursor and product ion mass tolerance of m/z 0.02 to create consensus MS² spectra. Then, to remove noisy data and data that were not reproducible, consensus spectra that contained fewer than two spectra were discarded. A network was then created where

edges were filtered to have a cosine score above 0.75 and more than five matched peaks. In addition, edges between two nodes were kept in the network only if each of the nodes appeared in each other's respective top 10 most similar nodes. The consensus MS² spectra in the network were then searched against spectral libraries in GNPS. The library spectra were filtered in the same manner as the input data. All matches kept between network spectra and library spectra were required to have a score above 0.75 and at least five matched peaks; 141275 MS² spectra were submitted to GNPS, of which 108118 were included in the molecular network. Those 108118 spectra were consolidated into 9644 consensus MS² spectra displayed as nodes in the full molecular network (Figure S2A). Consensus MS² spectra can be used as a proxy measure of the number of chemicals detected using untargeted MS; however, overestimation is likely as the same chemical can form different ion species in the instrument (e.g., $[\text{M} + \text{H}]^+$ and $[\text{M} + \text{Na}]^+$) as well as isotopologues (e.g., $[\text{C}_6\text{H}_6\text{O}_6 + \text{Na}]^+$ and $[\text{C}_6\text{H}_6\text{O}_6 + \text{Na}]^+$), which results in additional consensus MS² spectra. Then, 2.07% of consensus MS² spectra (200 of 9644) (Figure S2B) were annotated via GNPS, which corresponded to 77 unique chemicals (including the previously mentioned drugs). The rate of annotation is not uncommon in untargeted MS experiments of sample types less frequently investigated, in spite of using GNPS, which aggregates nearly all publicly accessible reference spectra. The molecular networking job is public (<https://gnps.ucsd.edu/ProteoSAFe/status.jsp?task=bbee697a63b1400ea585410-fafc95723>).

Source Tracking of GNPS-Annotated Chemicals and Differential Association Testing. The spectral library search function in GNPS, an integrated component of molecular networking, was used to annotate consensus MS² data. Annotated chemicals were tabulated as detected (i.e., 1) or not detected (i.e., 0) in each sample and output as a matrix, dubbed the chemical occurrence matrix. In parallel, the GNPS annotations were compiled into a manually curated source information table provided as Supporting Information. Annotated molecules were traced to a putative origin, i.e., source tracking, using heuristic or empirical information from published literature and chemical databases (e.g., PubChem). The chemical occurrence matrix and source information table were subsequently combined and processed in R. Annotations to the same chemical in the chemical occurrence matrix were collapsed into a single entry prior to data analysis. Multiple annotations for the same chemical can occur, often based on slight differences in the MS² product ion spectra that match different library spectra for the same chemical. The chemical occurrence matrix was output from R as a .csv file (samples in rows by variables in columns with metadata prepended to the beginning of the data matrix). In addition, a new matrix containing the source-tracking information, termed the source-tracking matrix (annotations in rows by samples in columns), was output from R as a .csv file.

Differential association testing of the chemical annotations (provided by GNPS in the chemical occurrence matrix) and categorical metadata groups was performed using a Fisher's exact test. *P* values were corrected for multiple-hypothesis testing using the FDR method.²²

Molecular Cartography of MS² Data. The MS² source-tracking matrix (output from GNPS) was merged with metadata on a sample-by-sample basis in a Jupyter notebook in R. Additional metadata required for plotting data in 'ili, a

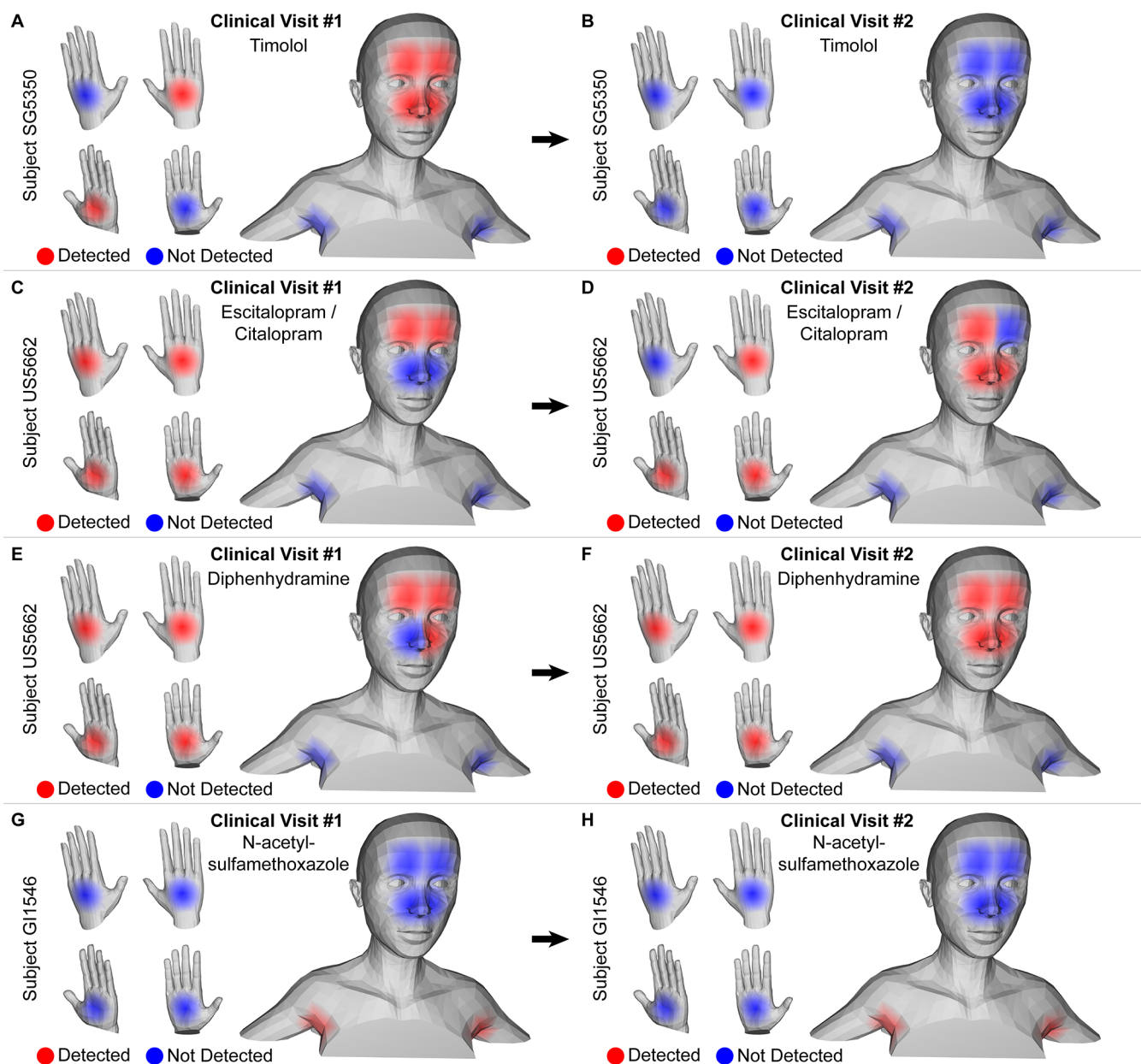


Figure 2. Illustrative 3D molecular cartography images depicting the locations at which drugs were detected (red) or not detected (blue) based on MS² spectral library matching in GNPS. Timolol in subject SG5350 during (A) clinical visit 1 and (B) clinical visit 2. Escitalopram/citalopram in subject US5662 during (C) clinical visit 1 and (D) clinical visit 2. Diphenhydramine in subject US5662 during (E) clinical visit 1 and (F) clinical visit 2. N-Acetyl-sulfamethoxazole in subject GI1546 during (G) clinical visit 1 and (H) clinical visit 2.

software for three-dimensional (3D) molecular cartography,²⁰ were added to the data–metadata table on the basis of the sample location (i.e., x , y , z coordinates and radii) on a 3D androgynous model of a human (.stl) downloaded from <http://nickzucc.blogspot.com/> (free download without copyright). The following parameters were used for orientation and visualization of the model: -112.62 , x -axis rotation; 22.1 , y -axis rotation; -135.81 , z -axis rotation; 2.5 , light; #575757, color; #ffffff, background; 1.0 , opacity; 0.05 , border opacity; and 1.0 , size factor.

RESULTS AND DISCUSSION

Detection of Drugs. Kidney transplant recipients are closely monitored, and multiple medications are frequently prescribed. In our cohort of 15 subjects, there were 75

prescribed medications, of which 12 were unlikely to be detected, viz., the elemental composition of K-Phos is not detected using our methods, via MS (rationale is given in Table S2). Fifty-eight of the 63 medications that can be detected had at least one reference MS² spectrum in the GNPS libraries that were used for annotation. GNPS was utilized to analyze the untargeted MS data, specifically MS² product ion scan, as the drugs and metabolites that could be detected via the skin were unknown. In addition, annotation based on comparisons between observed MS² fragmentation patterns and MS² reference spectra is more likely to be correct than relying on accurate mass measurement alone, particularly when chemical standards, e.g., drug metabolites, are not available or prohibitively expensive.

Eight prescribed drugs (escitalopram/citalopram, trimethoprim, mycophenolic acid, mycophenolate mofetil, diphenhydramine, dioctyl sulfosuccinate, timolol, and sulfamethoxazole) and one drug metabolite (*N*-acetyl-sulfamethoxazole) were annotated via GNPS in at least one sample. The annotations provided by GNPS spectral matching were supported by assessing the mass error between the mass of the precursor ion and the theoretical monoisotopic mass (<5 ppm error). The further rationale for annotation of the drugs is discussed in the [Supporting Information](#). Two additional drugs were detected, proguanil and dextromethorphan. Proguanil shares similar fragments with chlorhexidine (detected in samples), and it is believed to be a false positive or an in-source fragment of chlorhexidine as there was no record of antimalarial drugs. In addition, chlorhexidine is used in personal care products that are topically applied, such as hand soap, as an antibacterial agent, making this interpretation more plausible. Dextromethorphan was detected from only two swab samples from the hands of one subject. Although this was not on the patient's drug list, it is an over-the-counter drug that is widely available and exemplifies the advantage of an untargeted approach in combating the often poor reliability of self-reported drug use.

Molecular Cartography of GNPS-Annotated Drugs Indicates Drug-Specific Distributions. We used molecular cartography to visualize the spatiochemical (and temporal) relationship of the detected drugs ([Figure 2](#)). Chemical annotations from GNPS (MS^2 data), either detected or not detected, from all body locations are listed in [Table 1](#). A

Table 1. Numbers of Samples in Which a Drug Was Detected

annotated drug	axillary	face	hands
escitalopram/citalopram	0	5	7
dextromethorphan	0	0	2
trimethoprim	0	13	17
mycophenolic acid	0	0	2
<i>N</i> -acetyl-sulfamethoxazole	8	0	1
proguanil	2	8	22
mycophenolate mofetil	0	1	3
diphenhydramine	0	10	11
dioctyl sulfosuccinate	0	3	0
timolol	0	5	2
sulfamethoxazole	0	2	7

majority of annotated drugs were prescribed to the subject from which they were detected, providing a necessary positive control (exemplified by the following examples), supported by differential association testing via Fisher's exact test. Drugs were detected in different body locations that could reflect different mechanisms for their presence on the skin. Differential association testing results are listed in the [Supporting Information](#). Information about the drugs prescribed and detected is available in the [Supporting Information](#).

Timolol was detected on the face and hands of subject SG5350 during the first clinical visit ([Figure 2A](#)) but was not detected during the second clinical visit ([Figure 2B](#)), which could reflect the timing of application; however, the time of use prior to sampling was not available. Subject SG5350 was prescribed Combigan (brimonidine/timolol), an ophthalmic medication, used to treat glaucoma and ocular hypertension. It is postulated that the presence on the face and hands occurs as

a result of application to the eyes and transference to and from the hands to the surrounding forehead and nasolabial area.

In the case of drugs taken orally, we believe that the detection of drugs on the hands alone is more likely to result from transference (e.g., handling of pills) whereas detection on the face or axilla (and combinations of different body locations) is more likely to reflect drug elimination or transport to the skin. For example, escitalopram, a stereoisomer of citalopram (indistinguishable using our methods), was detected in the face and hand samples of subject US5662, the only subject prescribed citalopram ($p = 2.47 \times 10^{-14}$), during both clinical visits ([Figure 2C,D](#)). Citalopram, prescribed orally to this subject, is rapidly absorbed into systemic blood circulation and is lipophilic with high bioavailability. Citalopram is excreted in urine (12–23%) and feces (~10%) unchanged.²³ It is possible that escitalopram/citalopram is present on the skin as a result of diffusion (active or passive), sebaceous excretion, but it is also possible that escitalopram/citalopram is sequestered in dermal cells that eventually become part of the epidermis. Regardless of the mechanism, which cannot be conclusively determined in this study, the detection of escitalopram/citalopram on the skin supports the findings of our previous study⁴ in which citalopram was detected from the hand of a subject who self-reported consuming the drug.

Diphenhydramine, an antihistamine, was detected only in subject US5662, which matches the subjects' drug record ($p = 2.10 \times 10^{-14}$). Diphenhydramine was detected on the hands and face of the subject during both clinical visits ([Figure 2E,F](#)). Diphenhydramine is reported to be widely distributed in the body, metabolized extensively, and eliminated in urine.²⁴ Diphenhydramine and escitalopram/citalopram have similar theoretical logP values calculated in ChemDraw Professional (3.53 and 3.86, respectively), which could suggest they follow a similar mechanism.

While escitalopram/citalopram and diphenhydramine were prescribed and detected in only one subject, sulfamethoxazole was prescribed (in combination with trimethoprim, i.e., Bactrim SS) to all of the kidney transplant recipients per University of California, San Diego, protocol as prophylaxis for *Pneumocystis jiroveci* pneumonia. Sulfamethoxazole was annotated (based on MS^2) the following number of times per body location: zero, axilla; two, face; and seven, hands. This observation most likely results from transference during handling of the oral formulation; however, it is also possible that sulfamethoxazole is excreted onto or into the skin as it is known to be distributed in tissues and fluids in the body.²⁵ *N*-Acetyl-sulfamethoxazole, the major Phase II hepatic metabolite of sulfamethoxazole, was detected in one hand sample and eight axilla samples (illustrated in subject GI1546 in panels G and H of [Figure 2](#)). The observation of *N*-acetyl-sulfamethoxazole in the axilla compared to hands and face was statistically significant by differential association testing ($p = 2.29 \times 10^{-4}$). *N*-Acetyl-sulfamethoxazole was the only drug metabolite detected in the study through library matching (likely limited by the poor representation of drug metabolites in the MS^2 spectral libraries). A majority of sulfamethoxazole is converted into *N*-acetyl-sulfamethoxazole and excreted by the kidneys.²⁶ While we did detect *N*-acetyl-sulfamethoxazole, it was not detected in all individuals prescribed sulfamethoxazole. One rationale for these false negatives is that an MS^2 spectrum was not acquired due to a lack of signal intensity after dilution of axilla samples. It was necessary to dilute axilla samples prior to

analysis to avoid saturation of the detector caused by polypropylene glycol, present in some subject samples, which is believed to correspond to the use of personal care products (e.g., deodorants and antiperspirants).

The detection of *N*-acetyl-sulfamethoxazole in the axilla, a location of sweat glands (eccrine and apocrine), and known excretion of sulfamethoxazole in urine (theoretical logP of 0.57, ChemDraw Professional) suggest that *N*-acetyl-sulfamethoxazole might be secreted onto the skin via sweat. The detection of *N*-acetyl-sulfamethoxazole in locations different from those of sulfamethoxazole offers a strong contrast between the parent drug and metabolite. More generally, the observed differences might suggest that polar metabolites of drugs are more likely to be found in the axilla (and other locations of sweat glands) given that the major hepatic drug processes are oxidative and tend to yield more polar metabolites for renal excretion (as opposed to more nonpolar metabolites being excreted via the bile).

Concurrent Detection of Chemicals Important to Our Health. In addition to the detection of drugs, the untargeted MS approach provided information about other chemicals detected on the skin. Source-tracking information, i.e., the putative source of chemicals based on heuristic or empirical evidence, indicated a large number of chemicals categorized as environmental. Environmental exposure has a large impact on health. This information, provided at no additional cost via concurrent analysis with GNPS, could improve care particularly when used in conjunction with drug information.

Source-tracking information for annotated chemicals was categorized by body location (Figure S3 and Table S3). The proportion of each source category was similar between the skin of the face and hand but slightly different in the axilla samples with greater portions of annotations from environmental and multiple sources. The most represented source in each body location was the environmental category (e.g., ultraviolet protectants, phthalates, organophosphates, and biocides), which is notable yet not surprising as the skin is an environmental interface and humans exhibit a large number of behaviors that likely introduce chemicals (e.g., washing with soap and application of cosmetics and deodorants).

Fisher's exact test was used to test the differential association of annotated chemicals between the different body locations (as well as other metadata categories, e.g., gender). Dibutyl phthalate and dioctyl phthalate were differentially associated, statistically significantly, across different body locations (Figure S4). Dibutyl phthalate was detected more often in the axillary samples ($p = 2.58 \times 10^{-4}$), whereas dioctyl phthalate was detected more often on the face and hands of subjects ($p = 8.24 \times 10^{-16}$). Diethyl phthalate was also detected but lacked statistically significant differences between sample locations ($p = 0.271$). Phthalates are common chemicals in our environment and are common in cleaning products, deodorants, and makeup,²⁷ and detectable levels have been reported in human blood²⁸ and urine;²⁹ however, there is little information about the detection of phthalates via the skin.³⁰ Phthalates were not detected in all samples and are not believed to originate from sampling materials or analysis equipment as they are not present in the blanks. The observed differences in the locations of phthalates are hypothesized to reflect the application of different personal care products such as deodorant and makeup used on the axilla and face, respectively.

Triphenyl phosphate (a flame retardant and plasticizer) was detected on the hands more often than on the face and axilla

($p = 1.83 \times 10^{-4}$) (Figure S4) and might reflect a route of exposure, transference from objects to the hands and potential ingestion, which is supported by a previous study³⁰ (Figure S4). Benzalkonium chloride was observed on nearly 50% of all hand samples and detected more often on hands than on other body locations tested ($p = 4.05 \times 10^{-12}$). Similar to triphenyl phosphate, we hypothesize that our observations reflect transference from surfaces cleaned with quaternary ammonium biocides to the hands of subjects or application of personal care products.

CONCLUSIONS

The initial research toward developing a non-invasive MS method of monitoring drugs using the skin is presented. The exploratory goal in determining if drugs can be detected on the skin was accomplished. In summary, only a few of the prescribed drugs could be detected in the study. The two parent drugs that were clearly taken orally (escitalopram/citalopram and diphenhydramine) were observed in multiple skin locations on multiple days. We have concluded that the presence of these drugs most likely occurred via a systemic process; however, transference remains a possibility in lieu of a definitive mechanism. These drugs are lipophilic, and while they are not known to be present in or on the skin, there is prior knowledge that they are highly bioavailable and distributed in the body. We also detected timolol, a topically applied drug, supporting the idea that topical drugs can be detected using our methods and supporting prior MS studies of topical drugs.^{11–13} Finally, *N*-acetyl-sulfamethoxazole, an antibiotic metabolite, was detected in the axilla samples from subjects taking sulfamethoxazole. The detection of the hepatic metabolite confirms that sulfamethoxazole (taken orally) is simply not present on the skin via transference but uncharacterized pharmacokinetics to the skin may exist. We hypothesize the following potential mechanisms for the presence of drugs on the skin: passive diffusion or active transport from systemic blood circulation into the skin epidermis, secretion of molecules via sebaceous or sweat glands onto the epidermis, or sequestration in dermal cells that eventually become part of the epidermis. Regardless of the mechanism, the detection of drugs on the skin of subjects that have been prescribed drugs has not been previously reported.

We developed the ability to link GNPS annotations with putative source information via source tracking, which indicated a majority of annotated molecules on the skin originate from the environment as well as the multiple-source category (e.g., amino acids and lipids). Differential association testing indicated that specific molecules were present in different body locations with statistical significance, such as the presence of dibutyl phthalate in axilla samples or benzalkonium chloride in hand samples. Untargeted MS analysis of skin and data analysis via GNPS can provide insight into chemicals beyond drugs, for no additional effort, which might impact health, such as environmental chemicals present on the skin via direct application of personal care products, transference from cleaning products, etc.

On the basis of the results, qualitative drug monitoring (present or absent) is possible with the current method while the sensitivity and specificity could be improved by selecting which drugs intend to be monitored *a priori* and modifying the LC–MS method to more accurately and precisely acquire data for those drugs. Improvements in sensitivity may allow additional drugs, including those prescribed in this study that

were not detected, to be observed. In addition, the five bilaterally sampled locations evaluated in this study may have limited the number of drugs detected in this study. We cannot make a strong recommendation for sampling specific body locations for specific drugs, but we do believe that certain locations will be better than others for specific drugs. In addition, axilla and face samples are less likely to have contributions from transference compared to hand samples. The next stage of development is improving the ability to sample quantitatively and produce quantitative drug monitoring results, critical for some drugs. We envision the development of an accurate and precise sampling method that samples a fixed area of skin using a controlled amount of pressure and internal standards to correct for potential matrix effects. One challenge that exists is to establish drug levels in skin for which there is very little information available in the literature. Therefore, we plan to compare blood, urine, fecal, and skin drug levels in follow-up experiments to establish drug levels. While there are a number of crucial development steps that remain, the potential to reduce the inconvenience and morbidity of therapeutic drug monitoring by supplanting blood draws, to improve the methodology and cost of drug adherence testing, and to improve our understanding of drug pharmacokinetics is substantial.

■ ASSOCIATED CONTENT

📄 Supporting Information

The Supporting Information is available free of charge on the ACS Publications website at DOI: [10.1021/acs.analchem.8b05854](https://doi.org/10.1021/acs.analchem.8b05854).

Rationales for annotation, Figures S1–S6, and Tables S1–S3 (PDF)

Study metadata (TXT)

Chemical occurrence matrix (TXT)

Source-tracking matrix (TXT)

Differential association testing results (TXT)

Tabulated prescription drug information (TXT)

Tabulated detection of drugs (TXT)

■ AUTHOR INFORMATION

Corresponding Authors

*Clinical Aspects. Address: 9500 Gilman Dr., La Jolla, CA 92093-0657. Phone: 858-822-6629. E-mail: smtsunoda@ucsd.edu.

*Metabolomics Aspects. Address: 9500 Gilman Dr., La Jolla, CA 92093-0751. Phone: 858-534-6607. E-mail: pdorrestein@ucsd.edu.

ORCID

Alan K. Jarmusch: [0000-0002-2228-6308](https://orcid.org/0000-0002-2228-6308)

Pieter C. Dorrestein: [0000-0002-3003-1030](https://orcid.org/0000-0002-3003-1030)

Author Contributions

The manuscript was written through contributions of A.K.J., E.O.E., F.V., A.B., R.R.d.S., M.E., M.W., S.M.T., and P.C.D. A.K.J., E.O.E., F.V., K.K.d.R., and S.M.T. consented subjects or collected samples. A.K.J., E.O.E., and F.V. collected the data. A.K.J., R.R.d.S., M.E., M.W., S.M.T., and P.C.D. developed code or analyzed data. A.K.J., S.M.T., and P.C.D. designed the study.

Notes

The authors declare no competing financial interest.

■ ACKNOWLEDGMENTS

The authors thank all members of the Dorrestein lab, in particular, the contributions of staff members and Emily C. Gentry for the table of contents artwork. The authors also acknowledge the invaluable contributions of kidney transplant patients who voluntarily participated in this study. Funding for this work was provided by the following organizations: National Institutes of Health (S10-RR029121) and Office of Naval Research (N00014-15-1-2809). A.K.J. thanks the American Society for Mass Spectrometry for the 2018 Postdoctoral Career Development Award.

■ REFERENCES

- (1) Bouslimani, A.; Porto, C.; Rath, C. M.; Wang, M.; Guo, Y.; Gonzalez, A.; Berg-Lyon, D.; Ackermann, G.; Moeller Christensen, G. J.; Nakatsuji, T.; et al. *Proc. Natl. Acad. Sci. U. S. A.* **2015**, *112* (17), E2120–E2129.
- (2) Kapono, C. A.; Morton, J. T.; Bouslimani, A.; Melnik, A. V.; Orlinsky, K.; Knaan, T. L.; Garg, N.; Vázquez-Baeza, Y.; Protsyuk, I.; Janssen, S.; Zhu, Q.; Alexandrov, T.; Smarr, L.; Knight, R.; Dorrestein, P. C. *Sci. Rep.* **2018**, *8* (1), 3669.
- (3) Petras, D.; Nothias, L. F.; Quinn, R. A.; Alexandrov, T.; Bandeira, N.; Bouslimani, A.; Castro-Falcón, G.; Chen, L.; Dang, T.; Floros, D. J. *Anal. Chem.* **2016**, *88*, 10775–10784.
- (4) Bouslimani, A.; Melnik, A. V.; Xu, Z.; Amir, A.; da Silva, R. R.; Wang, M.; Bandeira, N.; Alexandrov, T.; Knight, R.; Dorrestein, P. C. *Proc. Natl. Acad. Sci. U. S. A.* **2016**, *113* (48), E7645–E7654.
- (5) Choi, M. J.; Oh, C. H., 2nd *Technology and Health Care* **2014**, *22* (3), 481–488.
- (6) Duffy, E.; Jacobs, M. R.; Kirby, B.; Morrin, A. *Exp. Dermatol.* **2017**, *26* (10), 919–925.
- (7) Reisdorph, N.; Armstrong, M.; Powell, R.; Quinn, K.; Legg, K.; Leung, D.; Reisdorph, R. J. *Chromatogr. B: Anal. Technol. Biomed. Life Sci.* **2018**, *1084*, 132–140.
- (8) Li, S.; Ganguli-Indra, G.; Indra, A. K. *Expert Rev. Proteomics* **2016**, *13* (5), 451–456.
- (9) Sadowski, T.; Klose, C.; Gerl, M. J.; Wójcik-Maciejewicz, A.; Herzog, R.; Simons, K.; Reich, A.; Surma, M. A. *Sci. Rep.* **2017**, *7* (1), 43761.
- (10) Dutkiewicz, E. P.; Chiu, H.-Y.; Urban, P. L. *Anal. Chem.* **2017**, *89* (5), 2664–2670.
- (11) Kijima, S.; Todo, H.; Matsumoto, Y.; Masaki, R.; Kadhum, W. R.; Sugibayashi, K. J. *Drug Delivery Sci. Technol.* **2016**, *33*, 157–163.
- (12) Sjövall, P.; Greve, T. M.; Clausen, S. K.; Moller, K.; Eirefelt, S.; Johansson, B.; Nielsen, K. T. *Anal. Chem.* **2014**, *86* (7), 3443–3452.
- (13) Bunch, J.; Clench, M. R.; Richards, D. S. *Rapid Commun. Mass Spectrom.* **2004**, *18* (24), 3051–3060.
- (14) Szekely-Klepser, G.; Wade, K.; Woolson, D.; Brown, R.; Fountain, S.; Kindt, E. J. *Chromatogr. B: Anal. Technol. Biomed. Life Sci.* **2005**, *826* (1–2), 31–40.
- (15) Gentili, S.; Mortali, C.; Mastrobattista, L.; Berretta, P.; Zaami, S. J. *Pharm. Biomed. Anal.* **2016**, *129*, 282–287.
- (16) Wang, M.; Carver, J. J.; Phelan, V. V.; Sanchez, L. M.; Garg, N.; Peng, Y.; Nguyen, D. D.; Watrous, J.; Kapono, C. A.; Luzzatto-Knaan, T.; et al. *Nat. Biotechnol.* **2016**, *34* (8), 828–837.
- (17) Sumner, L. W.; Amberg, A.; Barrett, D.; Beale, M. H.; Beger, R.; Daykin, C. A.; Fan, T. W.-M.; Fiehn, O.; Goodacre, R.; Griffin, J. L.; et al. *Metabolomics* **2007**, *3* (3), 211–221.
- (18) Pluskal, T.; Castillo, S.; Villar-Briones, A.; Orešič, M. *BMC Bioinf.* **2010**, *11* (1), 395.
- (19) Shannon, P.; Markiel, A.; Ozier, O.; Baliga, N. S.; Wang, J. T.; Ramage, D.; Amin, N.; Schwikowski, B.; Ideker, T. *Genome Res.* **2003**, *13* (11), 2498–2504.
- (20) Protsyuk, I.; Melnik, A. V.; Nothias, L.-F.; Rappez, L.; Phapale, P.; Aksenov, A. A.; Bouslimani, A.; Ryazanov, S.; Dorrestein, P. C.; Alexandrov, T. *Nat. Protoc.* **2017**, *13* (1), 134–154.

- (21) Scheubert, K.; Hufsky, F.; Petras, D.; Wang, M.; Nothias, L. F.; Dührkop, K.; Bandeira, N.; Dorrestein, P. C.; Böcker, S. *Nat. Commun.* **2017**, *8* (1), 1494.
- (22) Benjamini, Y.; Hochberg, Y. *Journal of the Royal Statistical Society: Series B* **1995**, *57* (1), 289–300.
- (23) Sangkuhl, K.; Klein, T. E.; Altman, R. B. *Pharmacogenet. Genomics* **2011**, *21* (11), 769–772.
- (24) Simons, K. J.; Watson, W. T. A.; Martin, T. J.; Chen, X. Y.; Simons, F. E. R. *J. Clin. Pharmacol.* **1990**, *30*, 665–671.
- (25) Kaplan, S. A.; Weinfeld, R. E.; Abruzzo, C. W.; McFaden, K.; Lewis Jack, M.; Weissman, L. *J. Infect. Dis.* **1973**, *128* (Suppl. 3), S547–S555.
- (26) Vree, T. B.; Hekster, Y. A.; Baars, A. M.; Damsma, J. E.; Van Der Kleijn, E. *J. Chromatogr., Biomed. Appl.* **1978**, *146* (1), 103–112.
- (27) Shen, H.-Y.; Jiang, H.-L.; Mao, H.-L.; Pan, G.; Zhou, L.; Cao, Y.-F. *J. Sep. Sci.* **2007**, *30* (1), 48–54.
- (28) Kato, K.; Silva, M. J.; Brock, J. W.; Reidy, J. A.; Malek, N. A.; Hodge, C. C.; Nakazawa, H.; Needham, L. L.; Barr, D. B. *J. Anal. Toxicol.* **2003**, *27* (5), 284–289.
- (29) Oktar, S.; Sungur, S.; Okur, R.; Yilmaz, N.; Ustun, I.; Gokce, C. *Minerva Endocrinol.* **2017**, *42* (1), 46–52.
- (30) Gong, M.; Zhang, Y.; Weschler, C. J. *Environ. Sci. Technol.* **2014**, *48* (13), 7428–7435.